OPTIMAL CONTROL LAWS FOR MICROBURST ENCOUNTER

Robert F. Stengel
Professor of Mechanical and Aerospace Engineering
Princeton University
Princeton, NJ 08544

ABSTRACT

Simplified structures for longitudinal control laws that reduce an aircraft's response to the strong head-tailwind and downdraft variations associated with microbursts are presented. They are based on non-zero-set-point linear-quadratic regulators that command throttle setting and angle of attack as functions of velocity and flight path angle, and they can incorporate direct measurements of the wind profile if available. Selection of cost functions to be minimized by feedback control has been aided by a prior study of classical control laws and exact nonlinear-optimal flight paths through realistic microburst wind profiles. The resulting optimal control laws have an adaptive, dual-mode structure that can be implemented either in flight-director logic or in an autopilot.

INTRODUCTION

Several recent aircraft accidents have resulted from attempts to takeoff or land through the severe wind condition known as a microburst. The phenomenon is best visualized as a vertically descending column of air that spreads out upon hitting the ground. In a typical scenario, the aircraft first experiences a headwind as it enters the outflow, causing the aircraft to balloon above the flight path if no corrective action is taken. Just as the pilot is throttling back to accommodate the headwind, it diminishes and is replaced by a downdraft, which is soon followed by a tailwind. The rapid loss of airspeed and the low energy state of the aircraft both contribute to a trajectory undershoot that can lead to ground impact.

In earlier papers [1-3], guidance strategies have been examined for both jet transports and general aviation aircraft that encounter microbursts. These include a classical control approach to flight control design [1], a survey of factors related to surviving such an encounter [2], and a study of exact optimal trajectories through known wind profiles [3]. These papers provide a firm foundation for the next phase of research.

Paper No. ICAS-86-5.6.3 for the 15th Congress of the International Council of the Aeronautical Sciences, London, England, September 1986.

Copyright © 1986 by ICAS and AIAA. All rights reserved.

This paper is an extension of the earlier work, in which realizable optimal control laws are developed for countering the wind shear. Whereas computation of the exact optimal controls requires perfect knowledge of the wind field before it is entered, the present development focuses on optimal control laws that use information collected up to the time of application [4], and they are based upon a simplified model of aircraft longitudinal dynamics. Thus, these new results provide an entry point for implementing control laws on actual aircraft, either as flight-director logic for manual piloting or in fully automatic systems. As before, both jet transport and general aviation aircraft are considered, The distinction is important because the two classes of aircraft tend to react differently to the microburst's components. (Typically, the jet transport has a more severe response to the head-tailwind shift, while the smaller, lighter aircraft has a larger adverse response to the downdraft.)

Optimal control dramatically improves an aircraft's ability to penetrate microbursts safely. Although avoidance remains the best policy, microbursts often give insufficient warning for such a strategy. Having encountered a microburst, optimal control provides the means for markedly improving the safety of flight.

PRIOR RESULTS

The longitudinal response of an aircraft to horizontal and vertical winds can be described by integrating a system of nonlinear ordinary differential equations that represent velocity, flight path angle, altitude, range, pitch rate, and pitch angle. Small perturbations from a nominal flight path obey linearized equations of motion, which possess modes of motion that are identified by the eigenvalues and eigenvectors of the linearized model. The modes of motion typically consist of long-period (phugoid) and short-period oscillations, as well as two pure integrations of the velocity vector to obtain altitude and range.

The phugoid mode arises from the aircraft's tendency to trade translational kinetic energy for potential energy (or velocity for altitude); hence, it is closely related to the aircraft's tracking of the flight path, a major concern in wind shear encounter. It is very lightly

damped and has a period that is proportional to airspeed. For airspeeds that are normally experienced during takeoff and landing (75 to 175 knots, depending on aircraft type), the phugoid period ranges from 17 to 40 sec. Thrust, drag, and lift, which are generated by throttle setting, flap and spoiler setting, and angle of attack (the angle between the aircraft's centerline and its velocity vector), are the principal control inputs for the mode.

The short-period mode describes angular motions of the aircraft about its center of mass, relative to an inertial frame of reference. It is controlled principally by the elevator, which is offset from the center of mass to generate a strong pitching moment. The short-period mode usually has a period of from one to five sec and is moderately well damped. The translational and angular motions of the aircraft occur on time scales that are roughly an order of magnitude apart. When viewed from the phugoid-mode time scale, the short-period mode appears to be in a quasi-steady state, its transient response to elevator inputs having died out long before significant translational motions occur. This attribute can be put to good use in examining guidance strategies for wind shear encounter, for it allows low-order dynamic models to be applied to the problem.

Using complete (6^{th}-order) longitudinal dynamic models as well as realistically lagged thrusting inputs, Reference 1 provided three important guidelines for designing control laws that desensitize an aircraft's response to vertical and horizontal wind shears. These guidelines are based upon Bode plots of altitude response to sinusoidal wind inputs, illustrated for a widely used 3-engine jet transport (JT) and a propeller-driven general aviation aircraft (GA) in Fig. 1:

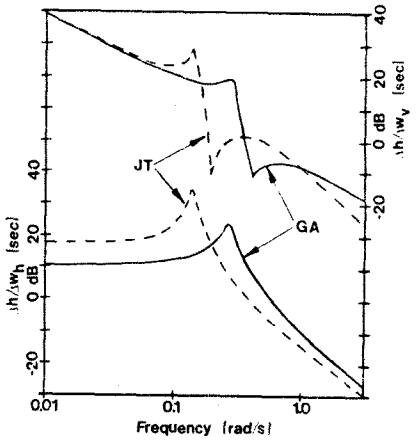

Figure 1. Open-loop frequency-response amplitude ratios for jet transport (JT) and general aviation (GA) aircraft [1].

1) Eliminate the resonant peak in the altitude response to horizontal wind shear at the phugoid natural frequency.

2) Eliminate the integration effect in the altitude response to downdraft.

3) Lower the altitude response to horizontal wind shear at all frequencies below the phugoid natural frequency.

The head-tailwind component that an aircraft experiences in traversing a microburst can be characterized as a single cycle of a periodic input. If that input has the same wavelength as the aircraft's lightly damped phugoid mode, it creates an amplified altitude deviation; this effect can be reduced by increasing the damping of the mode. In a steady downdraft, an uncontrolled aircraft picks up a downward velocity component that integrates into a net altitude loss; a properly designed control law can offset this tendency. Due to fundamental inertial properties, an aircraft has large-amplitude altitude response to low-frequency horizontal wind inputs and small-amplitude response to high-frequency inputs; closed-loop control can be used to attenuate the low-frequency response.

After examining a number of classical-control alternatives, closed-loop frequency responses such as those in Fig. 2 were obtained for the JT case. As shown in Fig. 3, these controllers greatly reduced the altitude excursions induced by a moderate level microburst in nonlinear simulation of the landing approach. Similar results were obtained in takeoff simulations; however, altitude excursions were greater because the aircraft was assumed to operate near full thrust, leaving little margin for thrust control against wind shear. Although linear control design techniques can be applied, the resulting control laws must be tested in an environment that includes the effects of thrust limiting and aerodynamic stalling of the aircraft's wing.

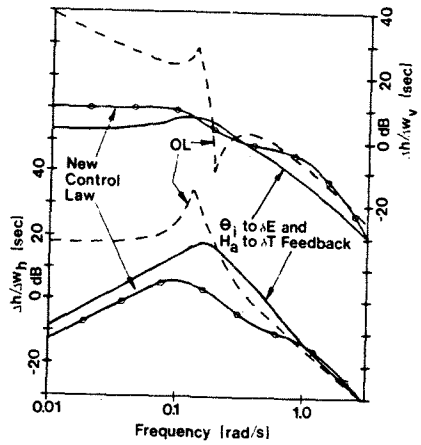

Figure 2. Comparison of open- and closed-loop frequency-response amplitude ratios for jet transport aircraft [1].

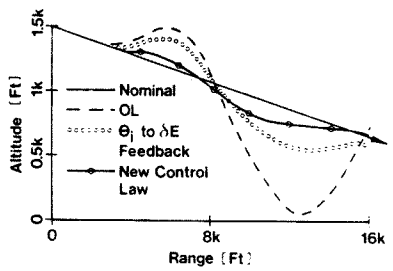

Figure 3. Comparison of open- and closed-loop transient response to nominal microburst [1].

Guidelines of a different sort were provided in Ref. 3, which reports on a study of optimal flight paths through microburst profiles. These flight paths are physically obtainable, but they were computed with the assumption that precise prior information of the wind profile could be used to frame the control strategy. As such, they provide a standard against which to judge implementable control laws, i.e., an indication of the true performance capabilities of the aircraft. Not surprisingly, a much better job of flight path tracking can be done when nonlinear numerical optimization is applied to the task. What was surprising was the degree of improvement that could be achieved: as shown in Fig. 4 and 5, it was possible for the JT model to fly through the most severe microburst profile yet identified in the Joint Airport Weather Studies (JAWS)[5]. While the controls-fixed flight path experienced a deviation from the landing approach path of about 1000 ft, negligible altitude excursions occurred with optimal control. Furthermore, neither the airspeed, angle of attack, nor throttle setting came close to exceeding normal operating limits.

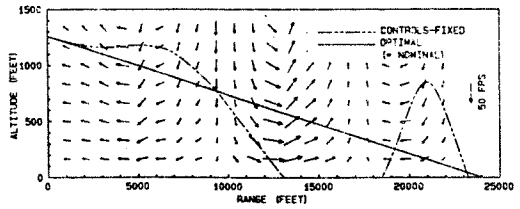

Figure 4. Controls-fixed and optimal flight paths of jet transport through the most severe JAWS head-tailwind shear [3].

Care should be exercised in interpreting these results, for it remains to be seen how close a practical control law can come to these results. Nevertheless, there are some lessons to be learned from this study. The most important is one that is easy to recognize in hindsight: to stay on the nominal path, the control should maintain lift equal to weight, even if this requires large variations in airspeed, angle of attack, and throttle setting. When airspeed was moderately penalized in the optimization cost function,

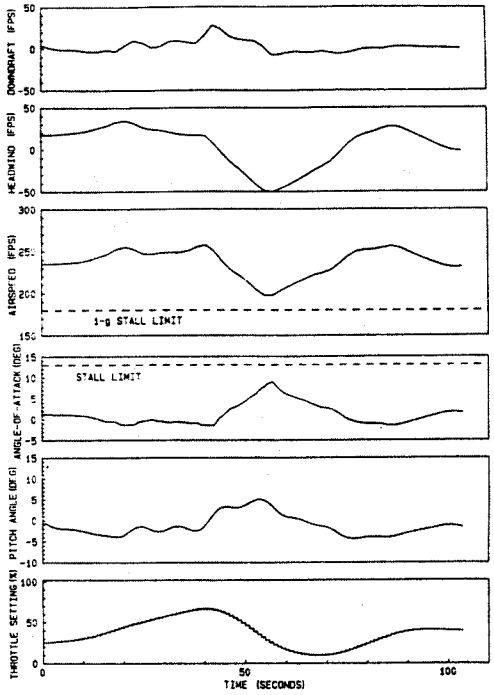

Figure 5. Time histories of input and output variables associated with optimal flight path of jet transport through the most severe JAWS head-tailwind shear [3].

large airspeed deviations occurred as lost lift was accounted for by increasing angle of attack. This behavior was due -- at least in part -- to the fact that the microburst was recognized as a discrete disturbance of finite length. The aircraft should be at something approximating nominal flight conditions when it comes out on the "other side" of the profile. When the penalty for airspeed deviations was made very large, airspeed tracking was greatly improved, but flight path tracking was degraded, reflecting the conflicting demands for pitch control. While airspeed was not totally neglected in either case, the throttle was seen to play a more important role in its regulation than in normal flight operations.

LONGITUDINAL EQUATIONS OF MOTION

Following Ref. 1, the aircraft's translational dynamic equations are written in an inertial frame fixed at the earth's surface (i.e., round, rotating-earth effects and short-period dynamics are neglected). The differential equations for inertial velocity (V_i), flight path angle (γ_i), and altitude above the surface (h) are as follows:

$$\dot{V}_i = [-qS[C_D\cos(\alpha_i - \alpha_a) + C_L\sin(\alpha_i - \alpha_a)] + T\cos\alpha_i)/m - g\sin\gamma_i \quad (1$$

$$\dot{\gamma}_i = [qS[C_L\cos(\alpha_i - \alpha_a) - C_D\sin(\alpha_i - \alpha_a)] + T\sin\alpha_i)/mV_i - g\cos\gamma_i/V_i \quad (2$$

$$\dot{h} = V_i \sin\gamma_i \quad (3$$

Here, T represents engine thrust, m is vehicle mass, S is the reference area for the lift and drag coefficients C_L and C_D, g is the gravitational constant, and q is the dynamic pressure, in which ρ represents air density:

$$q = (1/2)\rho V_a^2 \quad (4$$

The angles of attack in the inertial and air-relative frames are α_i and α_a, respectively; they are related by,

$$\alpha_a = \alpha_i + \gamma_i - \tan^{-1}\left(\frac{V_i \sin\gamma_i + w_V}{V_i \cos\gamma_i + w_H}\right) \quad (5$$

where w_V and w_H are the vertical and horizontal components of the wind. The airspeed V_a is related to the inertial velocity and the wind components by the following equation:

$$V_a^2 = V_i^2 + w_V^2 + w_H^2 + 2V_i(w_H \sin\gamma_i + w_H \cos\gamma_i) \quad (6$$

The lift and drag coefficients can be assumed to be linear and quadratic in α_a, respectively,

$$C_L = C_{L_o} + C_{L_\alpha}\alpha_a \quad (7$$

$$C_D = C_{D_o} + eC_L^2 \quad (8$$

with e reflecting the aerodynamic efficiency of the configuration.

While some rather large angular perturbations can be anticipated, they are likely to remain below 15 deg, so the usual small-angle assumptions would have maximum errors below 4 percent. In such case, the dynamic equations become

$$\dot{V}_i = (-qSC_D + T)/m - g\gamma_i \quad (9$$

$$\dot{\gamma}_i = (qSC_L + T\alpha_i - mg)/mV_i \quad (10$$

$$\dot{h} = V_i\gamma_i \quad (11$$

$$\alpha_a = \alpha_i + \gamma_i - \left(\frac{V_i + w_V}{V_i + w_H}\right) \quad (12$$

$$V_a^2 = V_i^2 + w_V^2 + w_H^2 + 2V_i(w_V\gamma_i + w_H) \quad (13$$

The present purpose is to develop locally linearized equations that can be used to investigate linear-quadratic optimal control laws; hence, these equations can be expanded about a nominal flight condition in Taylor series, dropping terms higher than first order and equating nominal solutions. The analysis is facilitated by assuming that nominal values of wind disturbances are zero, in which case $V_a = V_i$ and $\alpha_a = \alpha_i$ on the nominal flight path. Denoting perturbed variables by ^( ), air-relative velocity and angle-of-attack perturbations are,

$$\hat{V}_a = \hat{V}_i + \hat{w}_V\gamma_i + \hat{w}_H \quad (14$$

$$\hat{\alpha}_a = \hat{\alpha}_i + (\gamma_i\hat{w}_H - \hat{w}_V)/V_i \quad (15$$

allowing the linearized dynamic equations to be written as follows:

$$\dot{\hat{V}}_i = [-SC_D\rho V_N(\hat{V}_i + \gamma_N\hat{w}_V + \hat{w}_H) - q_N SC_{D_\alpha}\hat{\alpha}_a + \hat{T}]/m - g\hat{\gamma}_i \quad (16$$

$$\dot{\hat{\gamma}}_i = (SC_L\rho V_N(\hat{V}_i + \gamma_N\hat{w}_V + \hat{w}_H) + q_N SC_{L_\alpha}\hat{\alpha}_a + \alpha_N\hat{T} + T_N[\hat{\alpha}_a + \hat{w}_V - \gamma_N\hat{w}_H)/V_N])/mV_N \quad (17$$

$$\dot{\hat{h}} = \gamma_N\hat{V}_i + V_N\hat{\gamma}_i \quad (18$$

Note that the perturbation solution variables $(\hat{V}_i, \hat{\gamma}_i, \hat{h})$ are referenced to the inertial frame, whereas the angle of attack is referenced to the air-relative frame, recognizing the more natural definition for angle-of-attack measurements and control. In this simplified model, thrust and air-relative angle of attack serve as the control variables.

While this model can be applied to both jet-powered and propeller-driven aircraft, the thrust models for the two are different. For the former, thrust is largely independent of airspeed, and it is sufficient to consider $\hat{T}$ as the net controllable output of the engines. Propeller efficiency $E(V_a)$ varies with airspeed, and power P is the controllable output of a constant-rpm engine; hence, the thrust of the latter is best modeled as

$$T = E(V_a)P/V_a \quad (19$$

and its perturbation is sensitive to airspeed as well as throttle setting, here denoted as $\hat{P}$:

$$\hat{T} = T_V\hat{V}_a + T_P\hat{P} \quad (20$$

Consequently, the linearized equations for both aircraft types can be characterized in the form,

$$\begin{bmatrix}\dot{\hat{V}}\\ \dot{\hat{\gamma}}\\ \dot{\hat{h}}\end{bmatrix} = \begin{bmatrix}f_{11} & f_{12} & 0\\ f_{21} & 0 & 0\\ f_{31} & f_{32} & 0\end{bmatrix}\begin{bmatrix}\hat{V}\\ \hat{\gamma}\\ \hat{h}\end{bmatrix} + \begin{bmatrix}g_{11} & g_{12}\\ g_{21} & g_{22}\\ 0 & 0\end{bmatrix}\begin{bmatrix}\hat{Th}\\ \hat{\alpha}\end{bmatrix}$$

$$+ \begin{bmatrix}l_{11} & l_{12}\\ l_{21} & l_{22}\\ 0 & 0\end{bmatrix}\begin{bmatrix}\hat{w}_V\\ \hat{w}_H\end{bmatrix} \qquad (21$$

where the coefficients are derived from like terms in the linearized equations, unambiguous subscripts have been dropped, and ^Th represents throttle control. This is a special case of the linear differential equation,

$$\dot{\underline{x}} = F\underline{x} + G\underline{u} + L\underline{w} \qquad (22$$

where $\underline{x}$, $\underline{u}$, and $\underline{w}$ are the state, control, and disturbance vectors and F, G, and L are the stability, control-effect, and disturbance-effect matrices. Note that the third column of F and the third rows of G and L are zero, indicating that altitude perturbations have no dynamic effect on the state variables and that altitude is not directly affected by control or disturbances. We could, therefore, write this equation as,

$$\begin{bmatrix}\dot{\underline{x}}_1\\ \dot{\underline{x}}_2\end{bmatrix} = \begin{bmatrix}F_1 & 0\\ F_2 & 0\end{bmatrix}\begin{bmatrix}\underline{x}_1\\ \underline{x}_2\end{bmatrix} + \begin{bmatrix}G_1\\ 0\end{bmatrix}\underline{u} + \begin{bmatrix}L_1\\ 0\end{bmatrix}\underline{w} \qquad (23$$

where $\underline{x}_1$ contains ^V and ^Y, and $\underline{x}_2$ is ^h.

CONTROL STRUCTURES FOR MICROBURST ENCOUNTER

The control law should perform three functions:

- Provide proper command response
- Regulate against wind disturbances
- Assure satisfactory dynamic response

The first of these functions is achieved by designing the controller as a servo (or non-zero-set-point) regulator, where the set points corresponding to command inputs are independent of the feedback control law. The command inputs are determined by the pilot or autopilot, and while they may continuously change in time, they are assumed to be constant for design purposes. The second is affected by feedback gain selection, dynamic compensation, and (if available) feedforward of disturbance inputs. The third is a consequence of feedback gain selection and dynamic compensation.

Of course, overall system performance depends upon the control effectors and measurements that are available for closed-loop control. In the present paper, it is assumed that all necessary measurements can be made without error and that control is achieved by a combination of angle of attack and throttle setting or, once the throttle has saturated, by angle of attack alone.

Steady-State Command Response - It is appropriate to specify as many command inputs as there are independent controls (either one or two, as noted above). The command input $\underline{y}$ has a physical interpretation as a linear combination of state and control variables [6],

$$\underline{y} = H_x\underline{x} + H_u\underline{u} \qquad (24$$

Given a specific constant input $\underline{y}^*$, it is desired to find the corresponding equilibrium values of $\underline{x}^*$ and $\underline{u}^*$. These depend on the system's open-loop dynamics, and, since $\dot{\underline{x}} = 0$ at equilibrium,

$$0 = F\underline{x}^* + G\underline{u}^* + L\underline{w}^* \qquad (25$$

subject to the constraint specified by the command input, with $\underline{w}^*$ representing a constant disturbance. All objectives are satisfied by simultaneous solution of the two equations,

$$\begin{bmatrix}F & G\\ H_x & H_u\end{bmatrix}\begin{bmatrix}\underline{x}^*\\ \underline{u}^*\end{bmatrix} = A\begin{bmatrix}\underline{x}^*\\ \underline{u}^*\end{bmatrix} = \begin{bmatrix}-L\underline{w}^*\\ \underline{y}^*\end{bmatrix} \qquad (26$$

which leads to the following equation for $\underline{x}^*$ and $\underline{u}^*$:

$$\begin{bmatrix}\underline{x}^*\\ \underline{u}^*\end{bmatrix} = A^{-1}\begin{bmatrix}-L\underline{w}^*\\ \underline{y}^*\end{bmatrix} = B\begin{bmatrix}-L\underline{w}^*\\ \underline{y}^*\end{bmatrix}$$

$$= \begin{bmatrix}B_{11} & B_{12}\\ B_{21} & B_{22}\end{bmatrix}\begin{bmatrix}-L\underline{w}^*\\ \underline{y}^*\end{bmatrix} \qquad (27$$

where

$$B_{11} = F^{-1}(-GB_{21} + I) \qquad (28$$

$$B_{12} = -F^{-1}GB_{22} \qquad (29$$

$$B_{21} = -B_{22}H_xF^{-1} \qquad (30$$

$$B_{22} = (-H_xF^{-1}G + H_u)^{-1} \qquad (31$$

Of course, F must be invertable for this solution to exist, but as defined previously, the determinant of F is zero. This is an indication that there is no steady-state altitude perturbation $\hat{h}^*$ corresponding to non-zero values of $\hat{V}^*$ and $\hat{\gamma}^*$. The problem is easily solved by simply ignoring $\hat{h}$ in the calculation of the set point, i.e., by applying these equations to F_1, G_1, and L_1. It can be seen that the set point is sensitive to constant disturbance inputs as well as command inputs; hence, control system performance would be improved if disturbances could be taken into account directly.

Velocity and flight path angle are natural choices as command inputs, although velocity and altitude rate would be more in keeping with normal flight operations. Previous equations show that the choices are equivalent, as altitude rate is proportional to flight path angle when velocity is held constant. When throttle has saturated, one of the commands must be suspended; optimization results [3] suggest that flight path angle (or altitude rate) be retained as the single command input for control by angle of attack alone. Recalling that the microburst encounter is a transient phenomenon, velocity control can be resumed when the throttle is no longer saturated.

Servo Regulation - The control system should regulate about the set point, making it appropriate to consider linear control laws of the form

$$\tilde{u} = -C\tilde{x} \tag{32}$$

where the feedback gain matrix remains to be defined, and

$$\tilde{u} = u - u^* \tag{33}$$

$$\tilde{x} = x - x^* \tag{34}$$

Then the actual control is

$$u = u^* - C(x - x^*) \tag{35}$$

Using the relationships of the previous section to specify the set point, the control law becomes

$$\begin{aligned} u &= (B_{22} + CB_{12})\gamma^* - Cx - (B_{21} + CB_{11})w^* \\ &= C_\gamma \gamma^* - Cx - C_w w^* \end{aligned} \tag{36}$$

as shown in Fig. 6. The controller takes a very conventional structure; in the baseline case, C_γ is a (2 x 2) matrix converting the command inputs to control settings that account for feedback effects, and C is a (2 x 2) matrix that modifies system dynamics. If measurements or estimates of the disturbance are available, C_w is a (2 x 2) matrix that adjusts throttle setting and angle of attack for known (possibly changing) vertical and horizontal winds. For control by angle of attack alone, their dimensions are (1 x 1), (2 x 1), and (2 x 1), respectively. These structures are changed only slightly if integral compensation (discussed below) is incorporated.

Feedback Control Gains - Linear-quadratic (LQ) control theory provides a natural continuation of the previous study, allowing a direct interface between nonlinear-optimal flight path computations and implementable flight control laws. While it is quite feasible to synthesize digital control laws directly, (see, for example, Ref. 7), the proposed control concepts are most readily presented with continuous-time models and controllers. As shown in numerous texts and papers, minimization of the quadratic cost function,

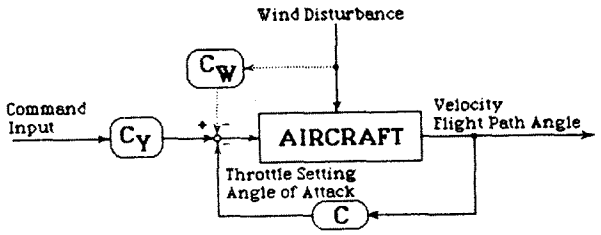

Figure 6. Linear-optimal control law for microburst encounter.

$$J = (1/2)\int_0^\infty [\tilde{x} \;\; \tilde{u}] \begin{bmatrix} Q & M \\ M^T & R \end{bmatrix} \begin{bmatrix} \tilde{x} \\ \tilde{u} \end{bmatrix} dt \tag{37}$$

subject to the dynamic constraint,

$$\dot{\tilde{x}} = F\tilde{x} + G\tilde{u} \tag{38}$$

leads to the control law,

$$\tilde{u} = -R^{-1}(G^T S + M^T)\tilde{x} \tag{39}$$

where S is the solution to an algebraic Riccati equation:

$$\begin{aligned} 0 = &-(F - GR^{-1}M^T)^T S - S(F - GR^{-1}M^T) + \\ &SGR^{-1}G^T S - Q + MR^{-1}M^T \end{aligned} \tag{40}$$

The principal design challenge is to choose values of the weighting matrices Q, M, and R that provide satisfactory closed-loop dynamic response, although it is reassuring that all such choices result in stable solutions as long as minimal criteria are satisfied [4]. One approach would be to use the same values used in Ref. 3, allowing for order reduction in the present case. A simpler approach is to recall the major conclusion of Ref. 3 -- control to maintain lift equal to weight -- recognizing that this renders flight-path-angle rate equal to zero. Accordingly, a state-rate weighting LQ regulator is obtained when Q, M, and R are defined as follows,

$$\begin{bmatrix} Q & M \\ M^T & R \end{bmatrix} = \begin{bmatrix} Fr_2^T \\ Gr_2^T \end{bmatrix} [Fr_2 \; Gr_2] \qquad (41$$

with Fr_2 and Gr_2 representing the second rows of F_1 and G_1, respectively. (These definitions are adjusted accordingly when angle of attack is the only control.) Note that even though this cost function is motivated by minimizing excursions in flight path angle rate, it provides weighting on velocity perturbations but no weighting on flight path angle itself. Furthermore, it introduces cross-product weighting on velocity in combination with throttle setting and angle of attack. The weighting matrices are completely specified without arbitrary parameters; however, there is freedom to emphasize certain elements of response, e.g., flight path angle tracking or relative use of the two controls, by extra weighting in Q or R.

Integral Compensation - Even though microburst encounter is a transitory phenomenon, it may be advantageous to penalize long-term deviations from the commanded input due to steady winds or parameter uncertainty. Integral compensation provides this feature, adding a slowly varying control bias against these effects. Defining the integral of the command input, $\underline{z}$, as,

$$\underline{z} = \underline{z}_o + \int_o^t [\underline{y}^* - H_x\underline{x} - H_u\underline{u}]dt \qquad (42$$

the LQ regulator is designed for the augmented system,

$$\begin{bmatrix} \dot{\underline{x}} \\ \dot{\underline{z}} \end{bmatrix} = \begin{bmatrix} F_1 & 0 \\ H_x & 0 \end{bmatrix} \begin{bmatrix} \underline{x} \\ \underline{z} \end{bmatrix} + \begin{bmatrix} G_1 \\ H_u \end{bmatrix} \underline{u} \qquad (43$$

resulting in a control law of the form (Fig. 7)

$$\underline{u} = C_y\underline{y}^* - C_x\underline{x} - C_w\underline{w}^* + C_I\underline{z} \qquad (44$$

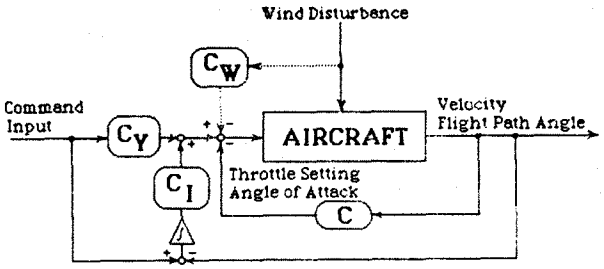

Figure 7. Linear-optimal control law with integral compensation for microburst encounter.

In the present case, strict control over velocity deviation during the microburst encounter is secondary, suggesting either that low weight be given to its integral or that its integral be ignored entirely. Recalling that this control law operates on inertial velocity while air-relative velocity is more important for long-term flight control, adding an airspeed-error integral at this point could be beneficial. Referring to the original equations, it is clear that incorporating the integral of flight path angle deviations is analogous to including altitude deviations in the dynamic model.

Conditions for Control Saturation - Referring to eq. 36, it is possible to obtain an estimate of the instantaneous wind effects that would drive the throttle and angle of attack to their limits. With zero command input and state feedback, the control would be specified by

$$\underline{u} = -(B_{21} + CB_{11})L\underline{w}^* \qquad (45$$

This represents two scalar equations, one for $\hat{}Th$, the other for $\hat{}\alpha$:

$$\hat{}Th = -c_{11}\hat{}w_V - c_{12}\hat{}w_H \qquad (46$$

$$\hat{}\alpha = -c_{21}\hat{}w_V - c_{22}\hat{}w_H \qquad (47$$

Replacing $\hat{}Th$ and $\hat{}\alpha$ by their maximum and minimum deviations from trim defines four straight lines in $(\hat{}w_V, \hat{}w_H)$ space; these are wind values that would saturate the controls, and they are seen to depend upon the value of the feedback gain C as well as on open-loop dynamics.

Dual-Mode Control, Anti-Windup, and Gain Scheduling - References 1 and 3 indicated that the throttle is likely to reach its limits before the aircraft stalls during microburst encounter. Therefore, it is appropriate to plan for the eventuality in which throttle is saturated and angle of

attack is the only remaining control. The suggested solution is dual-mode control, in which the two-control LQ regulator is used to the point of throttle saturation, and angle-of-attack-only LQ control is used beyond this point. While operating with saturated throttle, both control laws would be calculated, and the two-control version would be brought back on-line as soon as it commanded less than full throttle.

Integral compensators tend to "wind up" when controls are saturated, i.e., they build up unreasonable values when their commands go unheeded. This can lead to unacceptable undershoot after controls return to unsaturated levels. Consequently, integral terms should be zeroed when their corresponding control effectors have saturated.

Aerodynamic lift and drag are proportional to airspeed, which varies significantly during microburst encounter. This in turn affects the control system's optimal gains. Scheduling gains as a function of airspeed can preserve good system response over a wide range of flight conditions [7]. Consideration also could be given to adjusting gains to account for heavy rain, which often accompanies microbursts and is thought to degrade aircraft lift and drag characteristics.

Pilot Interface - In principal, the control logic presented here could be implemented in a fully automatic flight management system, and such systems will, no doubt, have anti-wind-shear features in the future. Velocity and flight path angle could be specified for the entire mission, leaving the flight crew to function primarily as system monitors. Nevertheless, there is good reason to assure that pilots have a system that can be "hand-flown" in hazardous conditions, even if the aircraft that the pilot flies is highly augmented. The pilot's ability to cope with the unexpected should be used to its fullest, and there is the important element of "controlling one's own destiny" in life-threatening situations. Therefore, it is important to examine control modes that retain the pilot "in the loop."

The control system presented here has at least two possible manual modes. The first is to allow the pilot to control velocity and flight path angle through conventional cockpit controls. Pilots have responded favorably to such systems in both ground-based simulation and flight test, but they are not in widespread use, so there is a problem of familiarity with procedures and expectations. The second alternative is to drive command bars and throttle "bugs" on flight director panel displays, giving the pilot the guidance he needs to do what the control system thinks best while reserving the capability to deviate from recommended control policy as he sees fit. Numerous human factors issues remain to be resolved in actual implementation.

CONCLUSION

Microbursts present a significant hazard for aircraft operations that is compounded by our present inability to detect them. When a severe microburst is detected, the prudent pilot will do his best to avoid flying in its vicinity; however, assistance should be given to the pilot who inadvertently encounters one. Prior studies indicate that aircraft typically have sufficient performance reserves to maintain nominal flight paths even in strong wind shears, although success depends critically on the control policies followed. The present study provides a framework for designing control systems that reduce flight path deviations caused by microbursts. Verification of this approach will be a topic for further study.

ACKNOWLEDGMENT

This work was sponsored by the Federal Aviation Administration and the National Aeronautics and Space Administration under Grant No. NGL 31-001-252.

REFERENCES

1. Psiaki, M.L., and Stengel, R.F., "Analysis of Aircraft Control Strategies for Microburst Encounter," AIAA Journal of Guidance, Control, and Dynamics, Vol. 8, No. 5, Sept-Oct 1985, pp. 553-559.

2. Stengel, R. F., "Solving the Pilot's Wind-Shear Problem," Aerospace America, Vol. 23, No. 3, Mar 1985, pp. 82-85.

3. Psiaki, M. L., and Stengel, R. F., "Optimal Flight Paths Through Microburst Wind Profiles," AIAA Paper No. 85-1833, Snowmass, CO, Aug 1985.

4. Stengel, R. F., STOCHASTIC OPTIMAL CONTROL: Theory and Application, John Wiley & Sons, New York, 1986.

5. Elmore, K.L., "JAWS Data Tape," National Center for Atmospheric Research, Boulder, CO, Feb 1985.

6. Stengel, R.F., "Equilibrium Response of Flight Control Systems," Automatica, Vol. 18, No. 3, May 1982, pp. 343-348.

7. Stengel, R.F., Broussard, J., and Berry, P., "Digital Flight Control Design for a Tandem-Rotor Helicopter," Automatica, Vol. 14, No. 4, July 1978, pp. 301-311.